

BRIEF DEFINITIVE REPORT

# A CMV-induced adaptive human V $\delta$ 1<sup>+</sup> $\gamma\delta$ T cell clone recognizes HLA-DR

Malte Deseke<sup>1,2</sup>, Francesca Rampoldi<sup>1</sup>, Inga Sandrock<sup>1</sup>, Eva Borst<sup>3</sup>, Heike Böning<sup>3</sup>, George Liam Ssebyatika<sup>4</sup>, Carina Jürgens<sup>3</sup>, Nina Plückerbaum<sup>3</sup>, Maleen Beck<sup>1,5</sup>, Ahmed Hassan<sup>1</sup>, Likai Tan<sup>1,6</sup>, Abdi Demera<sup>1</sup>, Anika Janssen<sup>1</sup>, Peter Steinberger<sup>7</sup>, Christian Koenecke<sup>1,5</sup>, Abel Viejo-Borbolla<sup>3,9</sup>, Martin Messerle<sup>3,9</sup>, Thomas Krey<sup>2,3,4,8,9</sup>, and Immo Prinz<sup>1,2,6,10</sup>

The innate and adaptive roles of  $\gamma\delta$  T cells and their clonal  $\gamma\delta$  T cell receptors (TCRs) in immune responses are still unclear. Recent studies of  $\gamma\delta$  TCR repertoire dynamics showed massive expansion of individual V $\delta$ 1<sup>+</sup>  $\gamma\delta$  T cell clones during viral infection. To judge whether such expansion is random or actually represents TCR-dependent adaptive immune responses, information about their cognate TCR ligands is required. Here, we used CRISPR/Cas9-mediated screening to identify *HLA-DRA*, *RFXAP*, *RFX5*, and *CIITA* as required for target cell recognition of a CMV-induced V $\gamma$ 3V $\delta$ 1<sup>+</sup> TCR, and further characterization revealed a direct interaction of this V $\delta$ 1<sup>+</sup> TCR with the MHC II complex HLA-DR. Since MHC II is strongly upregulated by interferon- $\gamma$ , these results suggest an inflammation-induced MHC-dependent immune response of  $\gamma\delta$  T cells.

## Introduction

The  $\gamma\delta$  TCR is the clonal antigen receptor expressed by  $\gamma\delta$  T cells. Whereas conventional  $\alpha\beta$  TCRs recognize peptides presented via the MHC I or II,  $\gamma\delta$  TCRs are considered to bind stress-induced surface molecules in an MHC-unrestricted manner. However, only a small and heterogeneous group of molecules has been described as ligands for  $\gamma\delta$  TCRs so far (Willcox and Willcox, 2019; Deseke and Prinz, 2020).

In humans, the largest fraction of  $\gamma\delta$  T cells in peripheral blood are V $\delta$ 2<sup>+</sup> and express a semi-invariant V $\gamma$ 9V $\delta$ 2<sup>+</sup> TCR (Delfau et al., 1992), which senses metabolic changes via so-called phosphoantigens (p-Ags), small nonproteogenic molecules with phosphate residues (Morita et al., 2007). P-Ags do not interact with the V $\gamma$ 9V $\delta$ 2<sup>+</sup> TCR directly but require the butyrophilins BTN2A1 and BTN3A1 to activate the receptor (Sandstrom et al., 2014; Rigau et al., 2020; Karunakaran et al., 2020). Since p-Ag stimulation is reminiscent of pattern recognition by innate receptors and induces a polyclonal expansion of V $\gamma$ 9V $\delta$ 2<sup>+</sup>  $\gamma\delta$  T cells, this reactivity has been defined as innate-like (Liuzzi et al., 2015; Fichtner et al., 2020). The more diverse non-V $\gamma$ 9V $\delta$ 2<sup>+</sup>  $\gamma\delta$  T cells are activated by a broad range of different host-cell derived antigens, such as EPCR (Willcox et al., 2012), Annexin A2 (Marlin et al., 2017), or EphA2 (Harly et al.,

2021). In particular, V $\delta$ 1<sup>+</sup>  $\gamma\delta$  T cells can recognize MHC-like molecules, e.g., CD1c (Roy et al., 2016), CD1d (Russano et al., 2006; Uldrich et al., 2013), and MR-1 (le Nours et al., 2019), largely irrespective of the presented lipid or metabolite antigen. Notably, also common MHC I molecules can be antigens for V $\delta$ 1<sup>+</sup>  $\gamma\delta$  TCRs, either in an allo-reactive fashion (Ciccone et al., 1989; Del Porto et al., 1994; Kierkels et al., 2019) or even peptide-specific, as was recently described for MART-1 (Benveniste et al., 2018).

Despite their low frequency at birth, non-V $\gamma$ 9V $\delta$ 2<sup>+</sup> including V $\delta$ 1<sup>+</sup>  $\gamma\delta$  T cells can expand clonally upon antigen exposure, which has led to the notion that this  $\gamma\delta$  T cell subset shows a more adaptive-like immune response (Ravens et al., 2017; Davey et al., 2017; Willcox and Willcox, 2019; Ravens et al., 2020). Here, we searched for ligands of V $\delta$ 1<sup>+</sup>  $\gamma\delta$  TCRs that had expanded in patients experiencing CMV reactivation after hematopoietic stem cell transplantation (HSCT; Ravens et al., 2017). We identified the MHC II variant HLA-DR as a cognate antigen for a V $\gamma$ 3V $\delta$ 1<sup>+</sup>  $\gamma\delta$  TCR. Although this HLA-DR recognition was not CMV peptide-specific, it underlines the general capability of  $\gamma\delta$  TCRs to recognize MHC molecules in immune responses.

<sup>1</sup>Institute of Immunology, Hannover Medical School, Hannover, Germany; <sup>2</sup>Excellence Cluster 2155 RESIST, Hannover Medical School, Hannover, Germany; <sup>3</sup>Institute of Virology, Hannover Medical School, Hannover, Germany; <sup>4</sup>Center of Structural and Cell Biology in Medicine, Institute of Biochemistry, University of Lübeck, Lübeck, Germany; <sup>5</sup>Department of Hematology, Hemostasis, Oncology and Stem Cell Transplantation, Hannover Medical School, Hannover, Germany; <sup>6</sup>Institute of Systems Immunology, University Medical Center Hamburg-Eppendorf, Hamburg, Germany; <sup>7</sup>Institute of Immunology, Medical University of Vienna, Vienna, Austria; <sup>8</sup>Center for Structural Systems Biology, Hamburg, Germany; <sup>9</sup>German Center for Infection Research, Partner Site Hamburg-Luebeck-Borstel-Riems, Hamburg, Germany; <sup>10</sup>Hamburg Center for Translational Immunology, University Medical Center Hamburg-Eppendorf, Hamburg, Germany.

Correspondence to Immo Prinz: [i.prinz@uke.de](mailto:i.prinz@uke.de).

© 2022 Deseke et al. This article is distributed under the terms of an Attribution-Noncommercial-Share Alike-No Mirror Sites license for the first six months after the publication date (see <http://www.rupress.org/terms/>). After six months it is available under a Creative Commons License (Attribution-Noncommercial-Share Alike 4.0 International license, as described at <https://creativecommons.org/licenses/by-nc-sa/4.0/>).

## Results and discussion

### Recognition of CMV-infected fibroblasts and B cell lymphoma cell lines by a V $\gamma$ 3V $\delta$ 1<sup>+</sup> $\gamma\delta$ TCR

Investigating the human  $\gamma\delta$  TCR repertoire after stem cell transplantation over time, we recently found via bulk TCR repertoire sequencing that in one of the investigated patients three V $\delta$ 1<sup>+</sup>-chains together with one V $\gamma$ 3<sup>+</sup>-chain were expanded in response to CMV reactivation (Ravens et al., 2017). Due to this simultaneous expansion of one V $\gamma$ - and three V $\delta$ -chains, we reasoned that the V $\gamma$  chain must have been shared by all three  $\gamma\delta$  TCRs. To validate this striking similarity between the three  $\gamma\delta$  TCRs termed TCR02, TCR04, and TCR05, we reassessed the original patient material by combined single-cell RNA (scRNA) and TCR sequencing. Indeed, this confirmed the presence and vast expansion of GZMB<sup>+</sup> FCGR3A<sup>+</sup>-activated effector  $\gamma\delta$  T cells expressing TCR02 and TCR05 but not TCR04 in blood samples taken after CMV reactivation (Fig. 1, A–C). Comparison of the CDR3 $\delta$  nucleotide sequences from the  $\gamma\delta$  TCR repertoire study revealed that TCR04 and TCR05 differed by only one nucleotide, which led to a switch in the amino acid at position 118 from glycine to valine (Fig. 1 D and Fig. S1 A). This suggested that the sequence of TCR04 was a serendipitous false positive variation of patient-derived TCR05 caused by a PCR error that has led to assume there was a substitution of glycine (TCR05) by valine (TCR04). Of note, the TCR04 TCR  $\delta$ -chain (TRD) sequence was also not found in datasets from other individuals or in public databases. Hypothesizing that the TRD-chain is key in mediating the binding of V $\delta$ 1<sup>+</sup>  $\gamma\delta$  TCRs, this may suggest that a similar  $\gamma\delta$  TCR rearrangement would not be selected under physiological conditions. Nevertheless, we included TCR04 in further screenings to assess potential effects of this amino acid exchange on antigen recognition.

To identify the ligands for TCR02, TCR04, and TCR05, we made use of a Jurkat (JE6.1) reporter cell line expressing GFP under the control of an NF- $\kappa$ B-specific promoter (Roskopf et al., 2016; Fig. 1 E). First, a JE6.1 TCR- $\beta$  knockout cell line (2G4) was generated and subsequently transduced with pairs of  $\gamma$ - and  $\delta$ -chain (Fig. S1 B). Next, we introduced the previously described CMV-induced V $\delta$ 1<sup>+</sup> TCR combinations and an innate V $\gamma$ 9V $\delta$ 2<sup>+</sup>  $\gamma\delta$  TCR as negative control into 2G4. To test for CMV reactivity in vitro, the transduced lines were cocultured with CMV-infected and noninfected fibroblasts. Of note, only the mutant TCR04 showed significantly increased reactivity towards CMV-infected fibroblasts but none of the patient-derived  $\gamma\delta$  TCRs (Fig. 1 F).

Since CMV-reactive  $\gamma\delta$  TCRs have been described to cross-react with tumor cells (Scheper et al., 2013), we next screened our 2G4 reporter cells expressing TCR02, TCR04, and TCR05 for reactivity with different leukemia cell lines. In particular, B cell lines (Raji, BL64) were recognized by related TCR04 and TCR05 but not by TCR02 and control V $\gamma$ 9V $\delta$ 2<sup>+</sup> TCR (Fig. 1, G and H), while monocytic cell lines like KG-1 and THP-1-stimulated TCR04 to a much lower extent. Interestingly, although K562 have been shown to activate V $\gamma$ 9V $\delta$ 2<sup>+</sup>  $\gamma\delta$  TCRs (Xiao et al., 2018), this was not the case in our experimental setting. A possible explanation might be that the used combination of CDR3 $\gamma$  and CDR3 $\delta$  in our V $\gamma$ 9V $\delta$ 2<sup>+</sup>  $\gamma\delta$  TCR is less favorable for this

stimulation. This would be in line with previous work by Wang et al. (2010) suggesting that the CDR3 influences p-Ag-mediated reactivity, the common means of activation of V $\gamma$ 9V $\delta$ 2<sup>+</sup>  $\gamma\delta$  TCRs.

### Identification of HLA-DR as antigen for TCR04 and TCR05

To characterize the binding of TCR04 and TCR05 to Raji cells, we generated soluble extracellular ectodomains of these  $\gamma\delta$  TCRs (sTCR) in insect cells and tetramerized them via a C-terminal Strep tag. In accordance with the coculture results, the tetramerized sTCR04 bound specifically to the Raji B cell line, whereas sTCR05 did not (Fig. 2 A). This suggests that the affinity of TCR05 for its antigen is too low for detection by sTCR staining albeit high enough for reporter cell activation. In contrast, the affinity of TCR04 towards its antigen was higher than usual  $\alpha\beta$  TCR affinities, as sTCR04 bound to Raji cells even in a monomeric form without previous tetramerization (Fig. 2 B). To identify the specific antigen recognized by TCR04, we made use of a genome-wide CRISPR/Cas9 knockout screening and selected those target cells, which lost the binding of TCR04 after transduction with the single guide RNA (sgRNA) library by FACS sorting (Fig. 2 C). In parallel to bulk next-generation sequencing after four rounds of selection, single clones of target cells negative for sTCR04 binding were generated and screened for contained sgRNAs. In line with the results from the Illumina sequencing of the bulk sorted cells (Table S1), HLA-DRA and transcription factors required for MHC II expression including RFXAP, RFX5, and CIITA were identified as relevant target genes (Fig. 2 D), indicating that HLA-DR is the cognate antigen of TCR04. To validate these results, we knocked out HLA-DR in Raji cells separately and observed that the reactivity was lost for both TCR04 and TCR05, but rescued upon re-expression of HLA-DRA (Fig. 2 E). This confirmed HLA-DR as a common ligand for related TCR04 and TCR05.

### Influence of the HLA-DRB haplotype and bound peptide on recognition by TCR04 and TCR05

HLA-DR comprises a high degree of combinatorial diversity of its  $\beta$ -chain. To address the influence of HLA-DR haplotype on the  $\gamma\delta$  TCRs' reactivities, HLA-DRB was selectively knocked out without affecting peptide loading as previously described (Crivello et al., 2019). This allowed for the selective recombinant expression of a subset of different HLA-DRB haplotypes that were screened for their activating capacity. All five tested haplotypes stimulated TCR04, whereas TCR05 did not respond to any tested haplotype. These included the haplotypes DRB1\*03 and DRB3\*02 endogenously expressed in Raji cells as well as DRB1\*11 and DRB1\*13, which were identified as the HLA-DR haplotypes of the original transplant/CMV patient (Fig. 3 A and Table S2). In contrast, reconstitution of HLA-DRB expression by CRISPR/Cas9-mediated homology-directed gene repair (HDR) restored recognition of HLA-DRB<sup>-/-</sup> cells by TCR04 and TCR05. Therefore, rescuing the phenotype in this cell line is possible (Fig. 3 B and Fig. S2 A), albeit not via transduction. We thus speculate that TCR05 requires another, yet unknown, signal beyond the mere presence of a specific HLA-DR haplotype, e.g., a preference for certain peptides, conformations, or glycosylation patterns. Moreover, recombinant overexpression of HLA-DRB

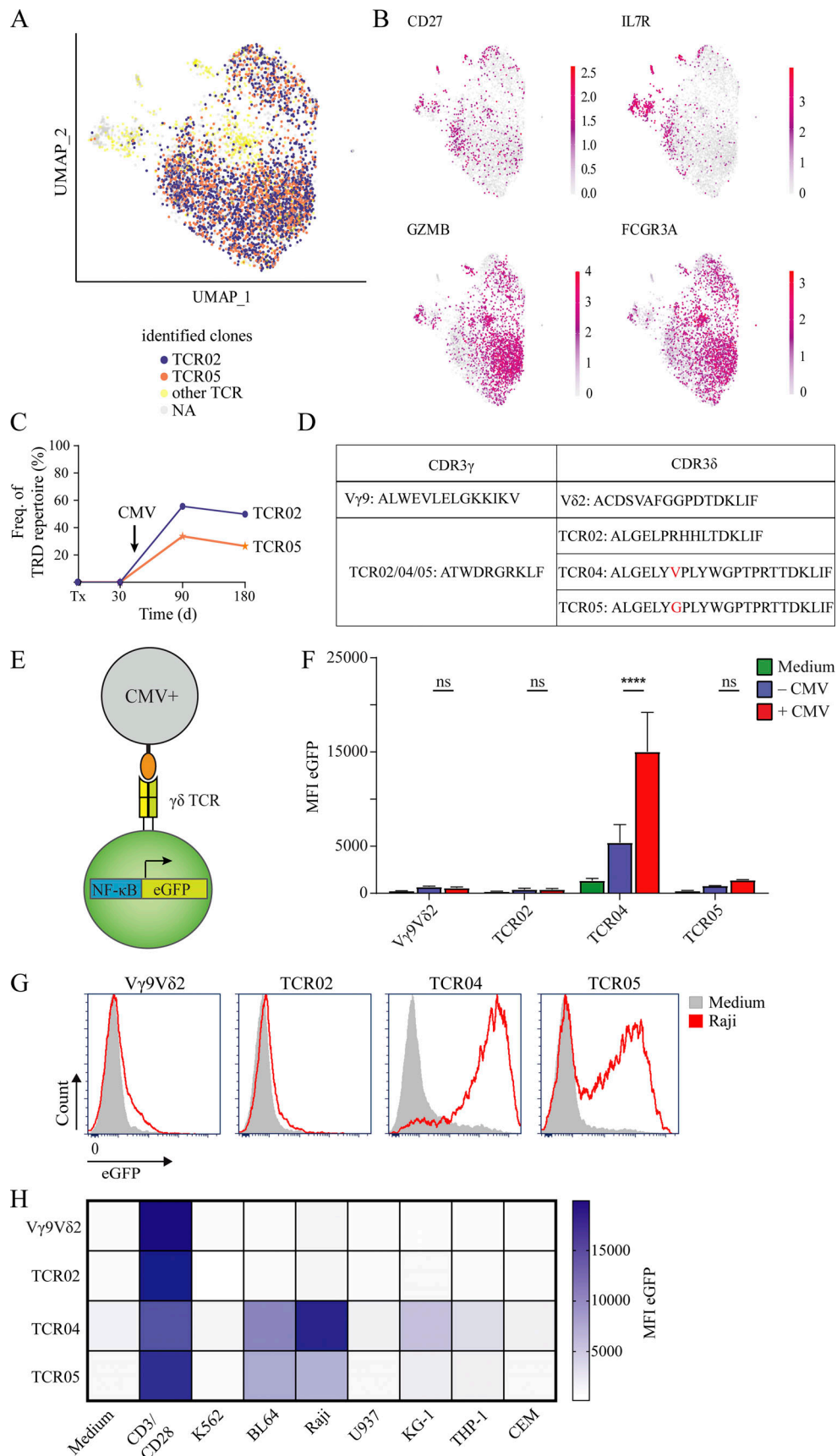


Figure 1. **Screening for reactivity of  $\gamma\delta$  TCRs.** (A)  $\gamma\delta$  T cells were FACS-sorted from frozen PBMCs and analyzed via single-cell sequencing. UMAP plot showing the distribution of expanded  $\gamma\delta$  TCR clones in an HSCT patient. (B) Expression of T cell maturation and activation markers by scRNA sequencing.

**(C)** Relative frequency of clones expressing TCR02 and TCR05 among the total *TRD* repertoire over time. **(D)**  $\gamma$ - and  $\delta$ -chain CDR3 sequences of TCR02, TCR04, and TCR05. The amino acid exchange between TCR04 and TCR05 is marked in red. **(E)** Schematic representation of the JE6.1 cells containing a reporter gene of GFP fused to an NF- $\kappa$ B-responsive promoter. **(F)** Reactivity of JE6.1 reporter cells expressing different  $\gamma\delta$  TCRs against CMV-infected fibroblasts defined as mean fluorescence intensity (MFI) of eGFP. Statistical test: two-way ANOVA with Tukey's multiple comparisons test; \*\*\*\*,  $P < 0.0001$  ( $n = 3-4$ , error bars = SD of mean). **(G)** Representative histograms of JE6.1 GFP fluorescence after coculture with Raji cells. **(H)** Heatmap of reactivity of JE6.1 reporter cells expressing TCR02, TCR04, TCR05, and the V $\gamma$ 9 $\delta$ 2 TCR towards leukemia cell lines. Each square represents the mean MFI of two to three independent experiments. Beads coated with TCR-engaging anti-CD3 and CD28 antibodies were used as a positive control. K562: erythromyeloblast; BL64 and Raji: Burkitt's lymphoma; U937/KG-1/THP-1: myeloid leukemia; CEM: T cell lymphoma cell lines. Coculture experiments were repeated  $n = 2-4$  times.

interferes with this signal and abrogates recognition by TCR05. The mutation in TCR04, however, abrogated this specificity as indicated by similar experiments with a peptide-loading-deficient Raji cell line (*RFXAP*<sup>-/-</sup>; Fig. S2 B). This was further confirmed by staining of JE6.1 cells expressing TCR02, TCR04, and TCR05 with HLA-DR tetramers presenting eight different peptides (Fig. S3). As Raji is a B cell lymphoma cell line, we assessed whether the requirements for activation of TCR04 and TCR05 can also be met by primary B cells from healthy donors or autologous B cells from the original transplant patient. Again, TCR04 was able to recognize all of the included B cell samples, whereas TCR05 and TCR02 were not (Fig. 3, E and F). Of note, both TCR02 and TCR05-expressing JE6.1 cells showed a slightly higher GFP expression upon coculture with autologous primary B cells, which is in line with their strong *in vivo* expansion the patient.

#### The $\delta$ -chain is decisive for the interaction with HLA-DR by TCR05

Although the comparison of TCR04 and TCR05 with the non-reactive yet very similar TCR02 suggested a major relevance of the CDR3 $\delta$  in HLA-DR recognition, a function of other CDRs could not be excluded. We therefore aimed at investigating the role of other domains of the  $\gamma\delta$  TCRs by generating CDR exchange mutants (Fig. 3 C). Furthermore, we included the hypervariable region 4 (HV4) in this screening, as it was recently described as the interaction interface for a group of  $\gamma\delta$  TCR ligands termed butyrophilin-like molecules (Melandri et al., 2018). We generated hybrid  $\gamma$ - and  $\delta$ -chains composed of either the CDR3 $\gamma$  of TCR05 in a V $\gamma$ 8-chain (TCR05\_V $\gamma$ 8\*) or the TCR05  $\delta$ -chain with CDR1, CDR2, or the HV4 being exchanged for the corresponding sequences from V $\delta$ 2 or V $\delta$ 3 sequences (TCR05\_CDR1 $\delta$ 3, TCR05\_CDR2 $\delta$ 2, TCR05\_HV4 $\delta$ 2). The exchange of the  $\gamma$ -chain had no impact on TCR05 reactivity towards HLA-DR, whereas it was completely lost upon exchange of CDR1 $\delta$  and CDR2 $\delta$  (Fig. 3 D). The HV4 hybrid TCR05 was responsive albeit with a lower magnitude, possibly due to structural constraints caused by the exchange. We therefore concluded that, although the  $\delta$ -chain CDR3 is a major prerequisite, CDR1 and CDR2 of the V $\delta$ 1-chain are equally required for the proper interaction of TCR05 and HLA-DR.

#### High affinity of $\gamma\delta$ TCR-HLA-DR interaction promotes trogocytosis towards the T cells

Surface plasmon resonance measurements quantified the direct interaction of TCR04 and TCR05 with HLA-DR. In line with previous coculture and sTCR staining experiments, the affinity of TCR04 towards HLA-DR was 86-fold higher ( $K_D = 32$  nM) than

the one of TCR05 ( $K_D = 2.7$   $\mu$ M; Fig. 4, A and B). Higher affinity of TCR04 towards the ligand led to stronger interaction with the leukemia target cells, as reflected in the transfer of cell surface molecules from the target to the T cell, a process termed trogocytosis (Li et al., 2019). Upon coculture of JE6.1 cells expressing TCR04 or TCR05 and Raji cells prestained with eFluor670, we observed a transfer of the dye towards the previously unstained JE6.1 cells, overall correlating with the GFP fluorescence detected after overnight coculture (Fig. 4 C). Also, JE6.1 reporter cells expressing TCR04 became positive for biotinylated proteins when cocultured for 5 min with surface-biotinylated Raji cells, confirming that transferred proteins originated from the cell surface (Fig. 4 D). Indeed, TCR04 activation by Raji cells led to an increase of HLA-DR on the JE6.1 cells, whereas this was not the case when Raji cells were *HLA-DR*<sup>-/-</sup>, indicating that the HLA-DR has not been expressed by the JE6.1 cells themselves (Fig. 4, E and F). However, the background HLA-DR transfer was high occurring also activation independently with TCR02. Therefore, higher affinity leads to increased cell-to-cell contact and hence to increased trogocytosis.

Since inflammatory cytokines such as IFN- $\gamma$  stimulate the expression of MHC II on many cell types (Maurer et al., 1987), we treated fibroblasts with IFN- $\gamma$  for 24 h. Indeed, increased expression of HLA-DR (Fig. 5 A) led to recognition by TCR04 but not by TCR05 (Fig. 5 B).

#### Tetramer staining confirms HLA-DR-reactive $\gamma\delta$ T cells in peripheral blood mononuclear cells (PBMCs)

To assess the frequency of HLA-DR-recognizing V $\delta$ 1<sup>+</sup>  $\gamma\delta$  TCRs, we stained magnetic-activated cell sorting (MACS)-isolated  $\gamma\delta$  T cells from 10 different individuals with HLA-DR tetramers. Since the exact role of HLA-DR haplotype and the presented peptide were still unclear for TCR05, we chose immediate early (IE)1 and IE2-derived peptides from CMV presented by HLA-DRB1\*03, with the latter one being endogenously expressed in Raji cells. To reduce the background staining due to the fluorochrome, we performed parallel staining with PE- and APC-labeled tetramers. Frequencies of HLA-DR tetramer double-positive V $\delta$ 1<sup>+</sup>  $\gamma\delta$  T cells ranged from 0 to 0.3% amongst all  $\gamma\delta$  T cells (Fig. 5, C and D). However, there were overall only few positive events and no clear population with a proportional staining for V $\delta$ 1<sup>+</sup>  $\gamma\delta$  TCR and HLA-DR tetramer was distinguishable. Therefore, and because the affinity of many HLA-DR-reactive  $\gamma\delta$  TCR including TCR05 may be too low for HLA-DR tetramer detection, it is still tempting to speculate that an inherent tendency for V $\delta$ 1<sup>+</sup>  $\gamma\delta$  TCRs to interact with MHC II molecules exists.

In early reports dating from more than 25 yr ago (Ciccione et al., 1989; Flament et al., 1994), reactivity of  $\gamma\delta$  TCRs towards

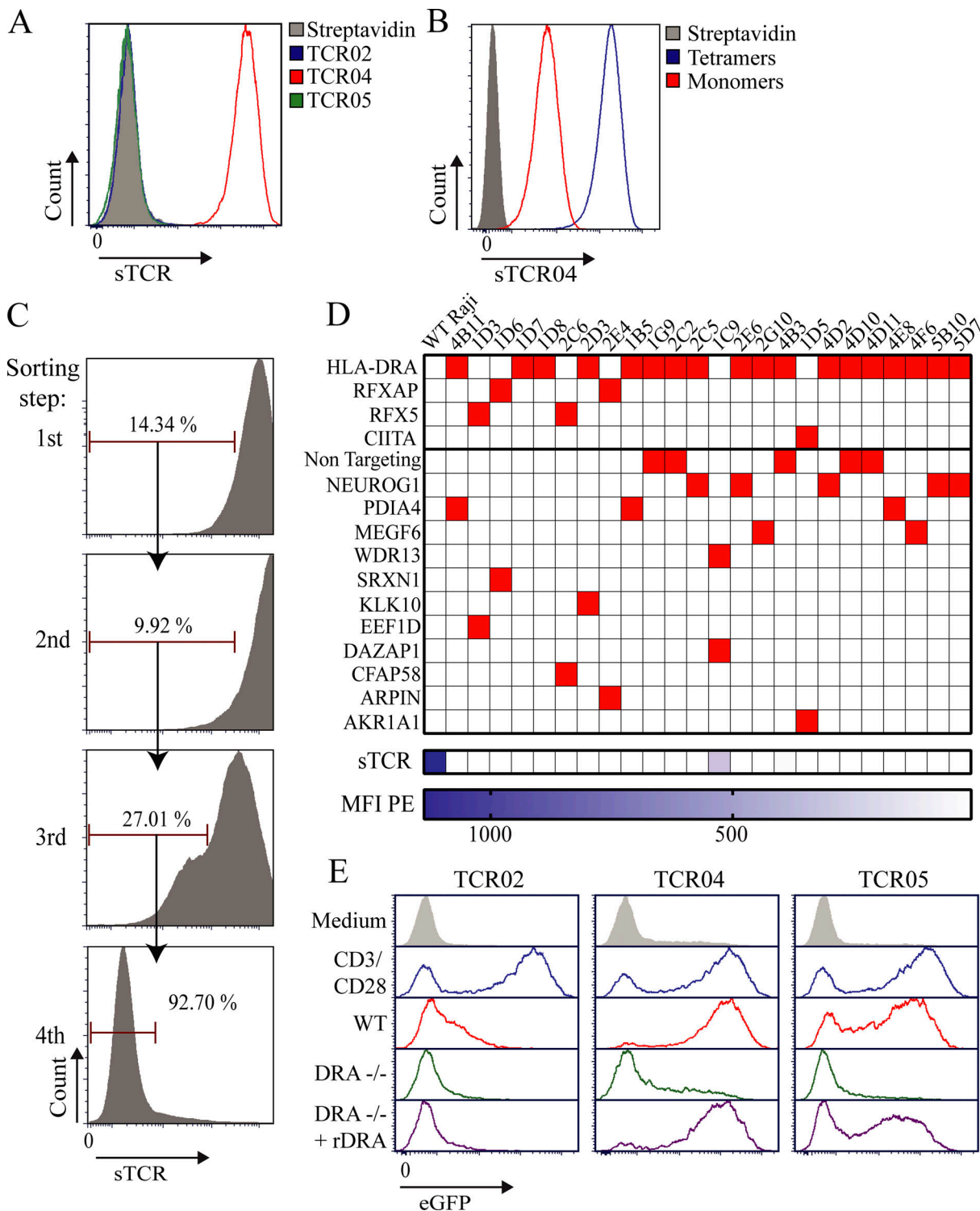
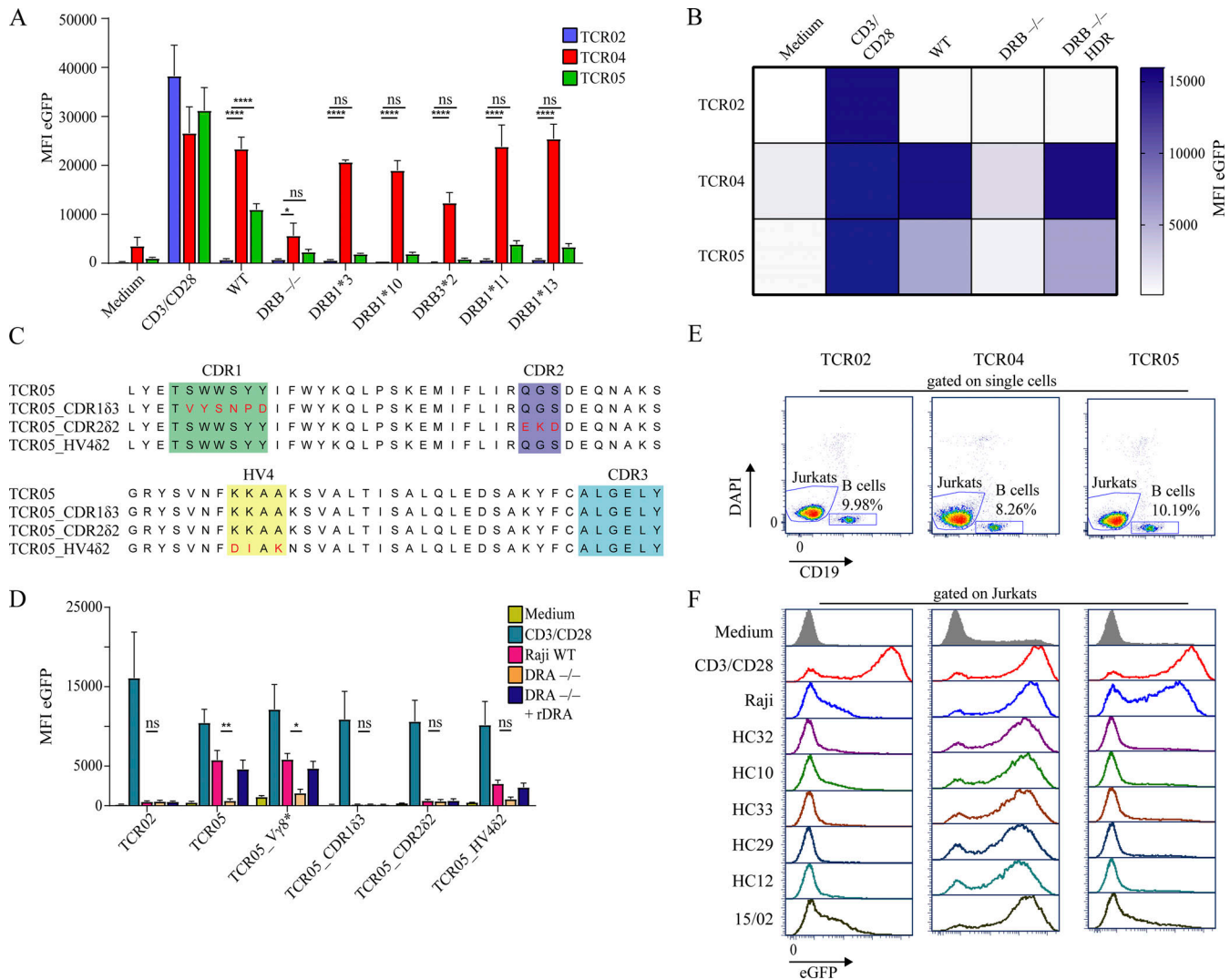


Figure 2. **Identification of HLA-DR as a ligand for TCR04 and TCR05.** (A) Staining of Raji cells with tetramers of TCR02, TCR04, and TCR05 (sTCR). Streptavidin-PE alone was used as a negative control. (B) Comparison of soluble TCR04 staining as tetramers and monomers. (C) Histograms indicate loss of TCR04 binding after consecutive sorting rounds in the genome-wide CRISPR/Cas9 knockout screening. 3 d after transduction with the CRISPR/Cas9 library, the Raji cells were stained with sTCR04 and the cells with the lowest staining were sorted four times for further subculture. (D) Analysis of subclones derived from the genome-wide CRISPR/Cas9 knockout screening for contained sgRNAs and sTCR binding. The horizontal axis depicts the generated clones, whereas identified target genes are given on the left vertical axis. Red squares indicate genes targeted by the respective sgRNAs and lower panels indicate the MFI. (E) Histograms showing eGFP fluorescence of JE6.1 cells expressing TCR02, TCR04, and TCR05 induced by coculture with different Raji cell lines. *DRA*<sup>-/-</sup>: HLA-DRA $\alpha$ -chain knockout (derived single-cell clone 1E11); 1E11 +DRA: HLA-DRA $\alpha$  knockout clone transduced with a transgenic HLA-DRA $\alpha$ -chain to rescue the phenotype. Cocultures and sTCR stainings were carried out  $n = 2-4$  times.



**Figure 3. Requirements for  $\gamma\delta$  TCR activation by HLA-DR.** (A) GFP fluorescence of JE6.1 cells cocultured with either Raji WT cells, the *HLA-DRB* knockout (*DRB<sup>-/-</sup>*), or *DRB<sup>-/-</sup>* transduced with a range of different DRB subtypes. Statistical test: two-way ANOVA with Tukey's multiple comparisons test; \*\*\*\*,  $P < 0.0001$  ( $n = 3$ , error bars = SD of mean). (B) MFI of eGFP of JE6.1 cells cocultured with either Raji WT cells, *DRB<sup>-/-</sup>* Raji cells, or *DRB<sup>-/-</sup>* with restored HLA-DRB expression by gene repair (HDR). Each square represents the mean MFI of two to three independent experiments. (C) Multiple alignment of TCR  $\delta$ -chain position 44–119. Compared are TCR05 with the CDR- and HV4-exchange mutants. (D) GFP fluorescence of JE6.1 cells expressing different hybrid versions or sequence chimeras of TCR05 with Raji cell lines. TCR05\_g8\*: a  $V\gamma 8$ -chain with the original CDR3 $\gamma$  from the TCR05. TCR05\_CDR1d: CDR1 exchanged with the  $V\delta 3$ -CDR1; TCR05\_CDR2d: CDR2 exchanged with a  $V\delta 2$ -CDR2; TCR05\_HV4d: HV4 exchanged with  $V\delta 2$ -HV4. Statistical test: two-way ANOVA with Tukey's multiple comparisons test; \*,  $P < 0.05$ ; \*\*,  $P < 0.005$  ( $n = 3$ , error bars = SD of mean). (E and F) Coculture of primary B cells with JE6.1 reporter cells expressing TCR02/04/05. After MACS isolation, primary B cells from five healthy donors and from an archived sample of patient 15/02, from whom TCR02/04/05 were identified, were cocultured with JE6.1 reporter cells expressing all three  $\gamma\delta$  TCRs at a ratio of 1:1. Separation of JE6.1 and B-cells via CD19 staining (E) and GFP reporter fluorescence of JE6.1 cells after coculture (F).

classical MHC molecules has been termed “allo-reactivity,” but later these studies were largely ignored as the paradigm emerged that  $\gamma\delta$  T cells are not MHC-restricted. This started to change with the more recent biochemical characterization of MHC I and MHC-like molecules as  $\gamma\delta$  TCR ligands (Benveniste et al., 2018; Kierkels et al., 2019; Uldrich et al., 2013), whereas recognition of MHC II has not been reported. Starting with the search for ligands of CMV-induced adaptive  $V\delta 1^+$   $\gamma\delta$  T cells, we recognized reactivity of a  $V\gamma 3V\delta 1^+$   $\gamma\delta$  TCR towards the MHC II variant HLA-DR on B cell lymphoma cell lines. The interaction is mainly mediated by the  $\delta$ -chain and involves all three CDRs. In

addition, we found that mutating the position 118 in the CDR3 $\delta$  from glycine to valine (TCR04) increased the affinity by two orders of magnitude, thereby allowing a general recognition of HLA-DR irrespective of the haplotype or presented peptides. In contrast, the preference of the original TCR05 for HLA-DRB haplotype or peptide remains unclear. Its reactivity in reconstituted *HLA-DRB<sup>-/-</sup>* cells was strongly dependent on the used target cell clone, suggesting the involvement of other factors in the antigen recognition process than the mere presence of HLA-DR. Secondary effects due to the transduction or gene repair process could be excluded, as the restoration of HLA-DR

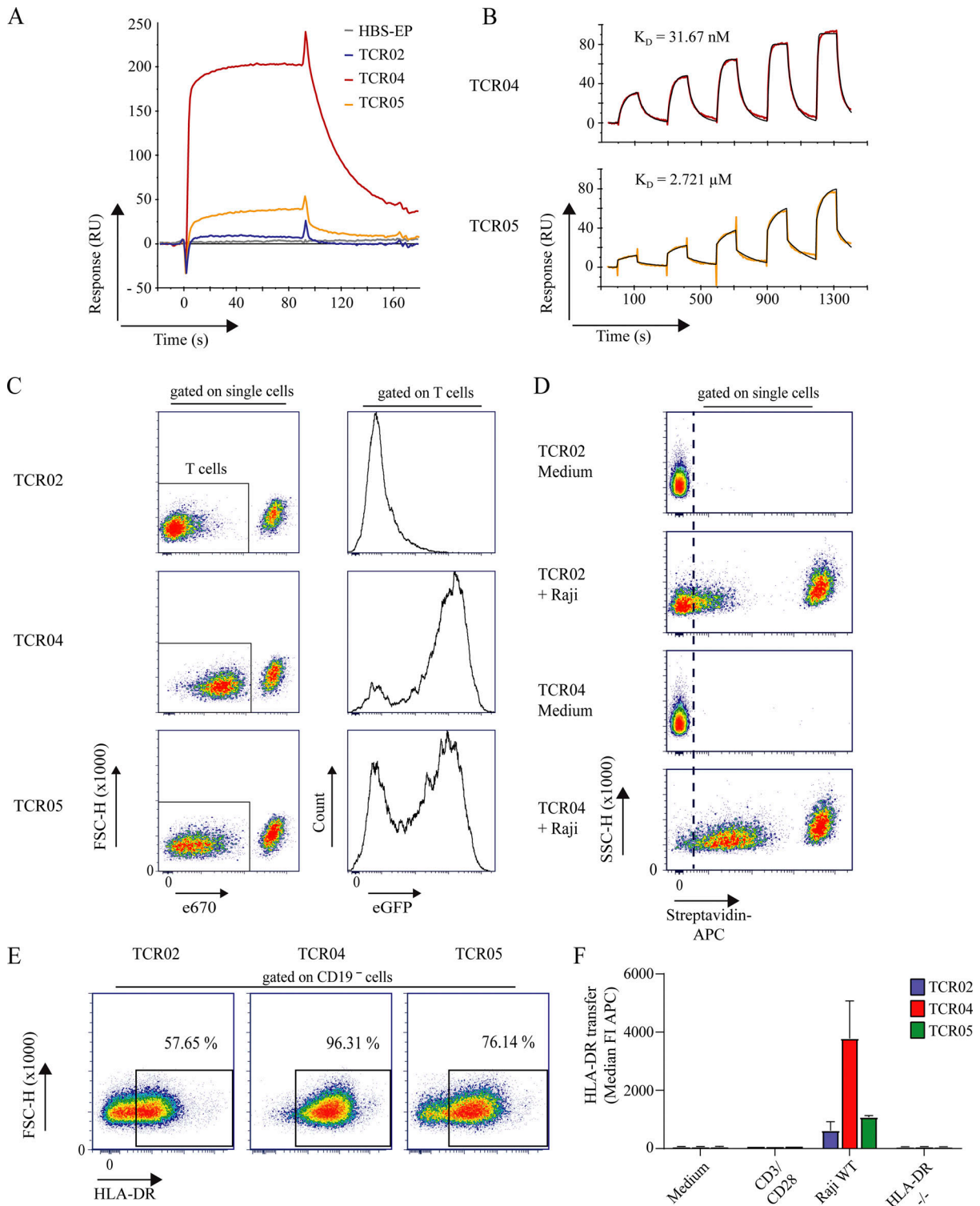


**Figure 4. Direct  $\gamma\delta$  TCR interaction with HLA-DR.** (A and B) Analysis of the interaction between TCR04 and TCR05 with HLA-DRB1\*03 presenting CLIP via surface plasmon resonance. (A) Sensorgram showing the interaction of injected TCR02, TCR04, TCR05 (2.5  $\mu\text{M}$ ), and HBS-EP (blank) with captured HLA-DR (capture level  $\sim 440$  RU). (B) Single-cycle kinetics of injected TCR04 (1:2 dilution ranging from 12.5 to 200 nM) over  $\sim 290$  RU captured HLA-DR and TCR05 (438–7,000 nM) over  $\sim 488$  RU captured HLA-DR. The curves were fit using a 1:1 binding model.  $n = 3$ . (C) Transfer of proliferation dye eFluor 670 upon  $\gamma\delta$  TCR activation. Dot plots show fluorescence of Raji cells prestained with eFluor 670 (e670<sup>high</sup>) and cocultured with JE6.1 cells expressing the indicated  $\gamma\delta$  TCRs (e670<sup>neg</sup> or 670<sup>low</sup>). Histograms show JE6.1 GFP fluorescence after 24 h of coculture, pregated on JE6.1 cells (T cells). The experiment was repeated at least three times. (D) Streptavidin-APC staining to detect transferred biotin after a coculture of  $\gamma\delta$  TCR-expressing JE6.1 cells with biotinylated Raji cells. (E) HLA-DR staining of JE6.1 cells expressing the indicated  $\gamma\delta$  TCRs after 5 min coculture with Raji WT cells. (F) Cumulative results of all HLA-DR transfer for all cocultured JE6.1 cell lines as median fluorescence intensity of HLA-DR-APC, gated on CD19<sup>-</sup>. All transfer experiments were repeated two times. Error bars represent SD of mean.

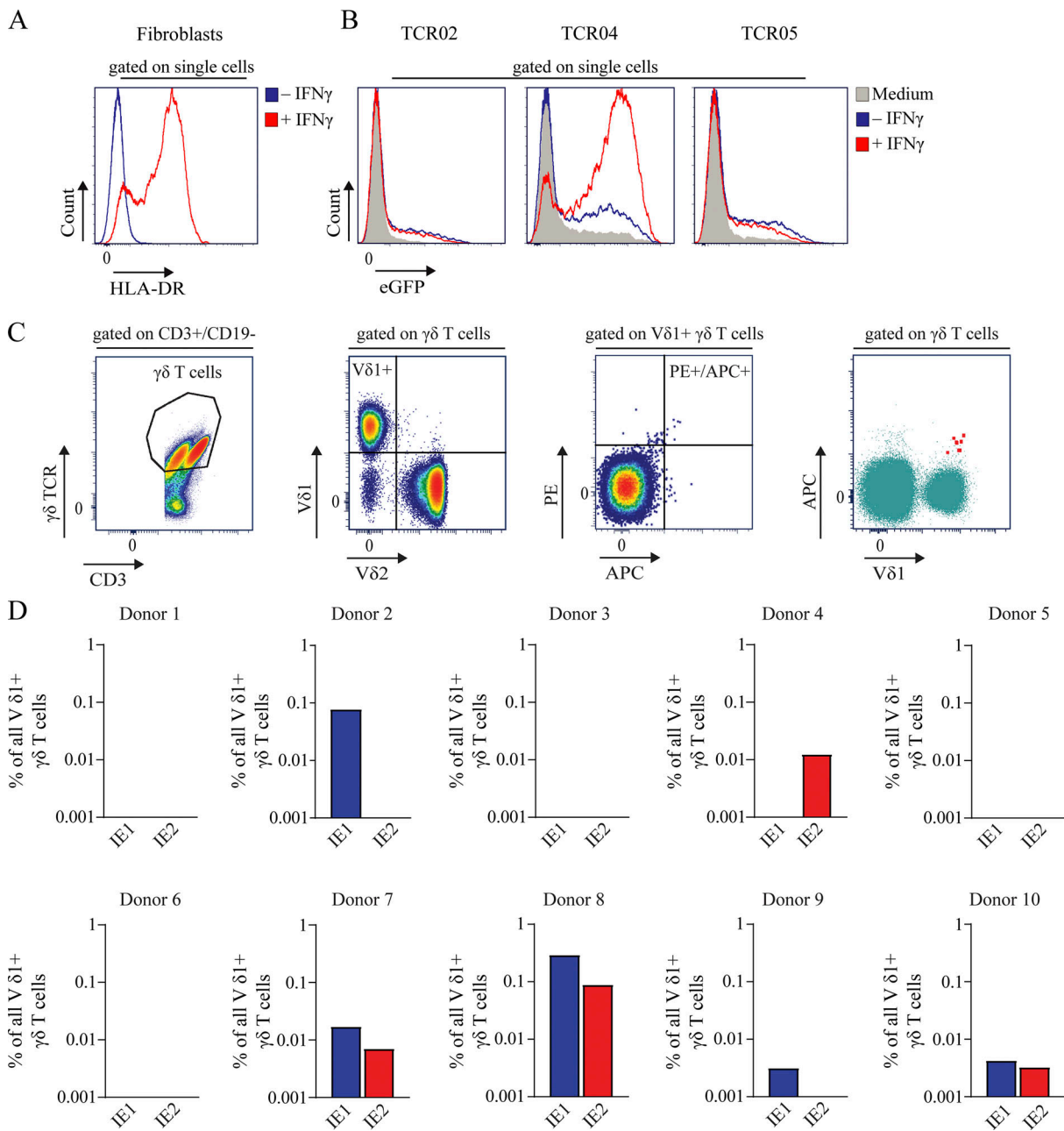


**Figure 5. Physiological context of HLA-DR recognition by  $\gamma\delta$  TCRs.** (A) Staining for HLA-DR expression on fibroblasts treated with recombinant IFN- $\gamma$ . (B) Coculture of JE6.1 reporter cells expressing TCR02, TCR04, or TCR05 with untreated fibroblasts or fibroblasts stimulated for 24 h with IFN- $\gamma$ . Medium with IFN- $\gamma$  was removed prior to the addition of reporter cells. (C and D) Parallel staining of  $\gamma\delta$  T cells from PBMCs with PE- and APC-labeled HLA-DRB1\*03 tetramers presenting CMV-derived peptides. (C) Representative dot plots gated on CD3<sup>+</sup>/CD19<sup>-</sup> (first left),  $\gamma\delta$  T-cells (second left and right), and V $\delta$ 1<sup>+</sup> (second right). PE<sup>+</sup>/APC<sup>+</sup> cells are highlighted in red in the right dot plot. (D) Frequencies of PE<sup>+</sup>/APC<sup>+</sup> (tetramer double-positive) cells. Presented peptide from CMV-encoded proteins IE1 or IE2 (for sequence details, see Fig. S3 C).

recognition by TCR05 worked well after either transduction or gene repair in some, but not all target cell clones. Recent reports on  $\gamma\delta$  TCR recognizing MHC I or MHC-like molecules suggested that these interactions are either independent of presented antigens (le Nours et al., 2019) or require a rather promiscuous range of peptides (Kierkels et al., 2019). In line with these observations, we speculate that also the interaction between TCR05 and HLA-DR may not rely only on a specific peptide but probably involves other factors such as conformation or

costimulators. This will, however, require further dedicated structural and functional analyses.

To which degree HLA-DR recognition can explain the CMV reactivity of the investigated clonotypes in the original patient has not been fully unraveled. Especially the unknown requirements for TCR05 activation aside the HLA-DR presence itself hamper final conclusions. Nevertheless, we hypothesize that CMV reactivation might have induced the expression of IFN- $\gamma$  by other immune cells leading to the expression of HLA-DR by



many hematopoietic cells, but also fibroblasts and epithelial cells, which might in turn have been recognized by the alloreactive V $\gamma$ 3V $\delta$ 1<sup>+</sup> TCR05 that was highly expanded in response to CMV reactivation.

Thus, despite the fact that  $\gamma\delta$  TCRs are considered as MHC-unrestricted, our findings add to the growing number of V $\delta$ 1<sup>+</sup>  $\gamma\delta$  TCRs that can recognize MHC or MHC-like molecules. Therefore, cognate interaction of V $\delta$ 1<sup>+</sup>  $\gamma\delta$  TCRs with MHC II molecules might be more common than so far expected. The supraphysiologic high affinity of the HLA-DR-reactive variant TCR04 requires further attention in the context of immunotherapeutic approaches involving  $\gamma\delta$  T cells and their TCRs.

## Materials and methods

### Human samples

Human blood samples were obtained from healthy individuals or HSCT patients with informed written consent. Experiments were performed in accordance with the declaration of Helsinki and approved by the institutional review board at Hannover Medical School (#1303-2012, #2032-2013, #2604-2014, and #2604-2015). PBMCs were isolated with Ficoll-Paque density-gradient media (GE Healthcare) and resuspended in PBS with 1% FCS for immediate use or frozen in RPMI with 10% FCS, 100 U/ml penicillin, 100  $\mu$ g/ml streptomycin sulfate, and 10% DMSO for long-term storage.

### Cell lines

The Jurkat reporter cell line JE6.1 NF- $\kappa$ B-eGFP was kindly provided by Peter Steinberger's lab in Vienna, Austria (Roskopf et al., 2016). The cell lines JE6.1, Raji, K562, U937, THP-1, KG-1, BL64, and CEM were cultivated in RPMI supplemented with 10% FCS, 100 U/ml penicillin, 100  $\mu$ g/ml streptomycin sulfate, 2 mM L-glutamine, and 1 mM sodium pyruvate (RPMI culture medium). HEK293T cells were maintained in DMEM (low-glucose) supplemented with 10% FCS, 100 U/ml penicillin, 100  $\mu$ g/ml streptomycin sulfate, and 4.5 g/liter glucose. The human fibroblast cell line hTERT-BJ-1 was kindly provided by Martin Meserle's lab and cultivated in a medium consisting of four parts of DMEM and one part of Medium 199 (Sigma-Aldrich) supplemented with 5% FCS, 1 mM sodium pyruvate, 2 mM glutamine, 100 U/ml penicillin, and 100  $\mu$ g/ml streptomycin sulfate. All cell lines were maintained at 37°C at a CO<sub>2</sub> concentration of 5% and tested regularly for mycoplasma contamination with the Mycoplasma Detection Kit (Lonza).

### Flow cytometry

PBMCs and cultured cells were washed with PBS + 1% FCS and up to 5  $\times$  10<sup>6</sup> cells per sample were stained with the following antibodies purchased from Miltenyi: anti-CD45-APC-Cy7 (clone: 5B1), anti- $\alpha\beta$  TCR-APC (clone REA562), anti- $\alpha\beta$  TCR-APC-Cy7 (clone: REA562), anti-CD3-PE-Cy7 (clone: SK7), anti- $\gamma\delta$  TCR-PE (clone: REA591), anti- $\gamma\delta$  TCR-APC (clone: REA591), anti-V $\delta$ 2 TCR-PerCP (clone: REA771), anti-CD19-Brilliant-Violet 605 (clone: SJ25C1), and anti-HLA-DRA-APC (clone: REA805). DAPI staining was used to discriminate living from dead cells when staining PBMCs. Fc-blocking of PBMCs was performed using

Human TruStain FcX (BioLegend). Samples were acquired with the BD LSRII flow cytometer. Analysis of the results was performed with FCS Express (Version 7.06.0015). If the stained cells were to be sorted, this was performed with the FACSaria Fusion at the Cell Sorting Facility of Hannover Medical School.

### Cloning

The cDNA sequences for the expression of  $\gamma\delta$  TCRs outside the CDR3 were obtained from the international ImMunoGeneTics information system (<http://www.imgt.org>) and the HLA-DR cDNA sequences were obtained from the Immuno Polymorphism Database. The CDR3 sequences for the TCR02, TCR04, and TCR05 were described in Ravens et al. (2017). The cDNA sequences were synthesized by BIOCAT and cloned into the retroviral Vectors pBulletIRESneo and pBulletIRESpuro (both vectors kindly provided by Jürgen Kuball's lab; University Medical Center Utrecht, Utrecht, Netherlands) via the restriction sites for NcoI and BamHI. For the soluble TCR expression, the extracellular domains of the respective  $\gamma\delta$  TCRs were amplified by PCR by using the NEBNext 2 $\times$  PCR Master Mix from New England Biolabs and the following primers: V $\gamma$ 3-forward: 5'-GAAGATCTTCCAGCAATCTGGAGGG-3'; V $\gamma$ 3-reverse: 5'-GCTCTAGACTGCAGCAGCAGGGTATC-3'; V $\delta$ 1-forward: 5'-GAAGATCTGCCAGAAAGGTGACCCAGG-3'; V $\delta$ 1-reverse: 5'-GCTCTAGACTTCTCTGTGTGCACGATGGC-3'.

The PCR product was cloned into the vector pT1205 (Krey et al., 2010) via the restriction sites XbaI and BglII. For the in silico design of CDR-exchange mutants, the CDR1 of V $\delta$ 1 was replaced by the CDR1 of V $\delta$ 3, the CDR2 of V $\delta$ 1 by the CDR2 of V $\delta$ 2, and the HV4 of V $\delta$ 1 by the HV4 of V $\delta$ 2. The  $\gamma$ -chain hybrid V $\gamma$ 8\_04\* was designed by replacing the CDR3 of a V $\gamma$ 8-chain with the CDR3 of the V $\gamma$ 3-chain of the TCRs 02, 04, and 05. The CDR-exchange mutants as well as the hybrid V $\gamma$ 8\_04\* were then synthesized by BIOCAT and cloned into the pBullet vectors, respectively.

### Generation of CRISPR/Cas9 knockout cell lines

For the generation of CRISPR/Cas9 knockout cell lines, Cas9 ribonucleoparticle preparation and transfection was performed as described elsewhere (Martens et al., 2020). In brief, the gene-specific CRISPR RNA (crRNA) was combined with tracrRNA (both obtained from IDT) to form the gRNA by heating them at 95°C. After cooling the sample down to room temperature, Alt-R CRISPR-Cas9 was added to form the ribonucleoparticles. The respective crRNAs were: TRB KO in JE6.1: 5'-GGCTCAAACACA GCGACCTC-3' (gRNA1), 5'-GGCTCTCGGAGAATGACGAG-3' (gRNA2, both described in Legut et al. [2018]); HLA-DRA KO in Raji: 5'-TGCATTGGCCAACATAGCTG-3'; RFXAP KO in Raji: 5'-ACACCGCAACAAGATGTACA-3'; HLA-DRB KO in Raji: 5'-GAG TACTGGAACAGCCAGA-3' (as described in Crivello et al. [2019]).

For Jurkat cell nucleofection, the SE cell line nucleofection kit was used, and for Raji cells, the SG cell line nucleofection kit was employed. The cells were cultivated for a week and sorted for negative cells by flow cytometry and subsequently single-cell clones were generated by limiting dilution. Here, the cells were diluted to reach a density of 5 ml<sup>-1</sup>. The cell suspension was

distributed over 96-well plates with 100  $\mu$ l per well and incubated for 2 wk. The obtained clones were screened for the respective knockout by antibody staining.

#### Gene repair of HLA-DRB knockout cell lines via HDR

To repair the mutation inserted into the HLA-DRB gene by CRISPR/Cas9, gene knockin via HDR was employed. In brief, a gRNA cutting 13-bp upstream of the previously mutated region was used to introduce a double-strand break as described in the previous section. In parallel, a single-stranded DNA (ssDNA) oligomer with homology arms up- and downstream of the cutting site was added to allow for the HDR. After culturing the cells for 1 wk, rescue of HLA-DR gene expression was determined via flow cytometry.

The respective crRNA was: 5'-GGCGGCTGATGCCGAGTAC-3'.

The ssDNA oligomer was: 5'-TTCGACAGCGACGTGGGGGAGTTCCGGGCGGTGACGGAGCTGGGCCGCCAGACGCCGAATATTGGAACAGCCAGAAGGACCTCTGGAGCAGAAGCGGGGCCGGTGGACAACACTACTGCA-3'.

Both, crRNA and ssDNA oligomer were purchased from IDT and designed using the Alt-R HDR Design tool from IDT.

#### Retroviral transduction

For retroviral particle production,  $2 \times 10^6$  HEK293T cells were seeded in two 10-cm<sup>2</sup> plates and cultured overnight. The following day, the cells were calcium chloride transfected with the respective pBullet-plasmid, the env-plasmid pMD2.G\_VSVg, and the gag-pol-plasmid pCDNA3.1MLVwtGag/Pol (both kindly provided by the Department of Prof. Dr. Axel Schambach, Department of Hematology, Hannover Medical School, Hannover, Germany). For the transfection, the CAPHOS kit from Sigma-Aldrich was used. The supernatant of the cultures was harvested the next 2 d and the viral particles were subsequently concentrated by ultracentrifugation overnight. Transduction of JE6.1 and Raji cells was performed by spin infection for 2 h with 4-nM protamine sulfate and 20  $\mu$ l of each viral particle suspension to be transduced. After an incubation of 2 d and medium renewal, the cells were selected for successful transduction with 1-ng/ $\mu$ l puromycin and/or 600 ng/ $\mu$ l G418 for 1 wk. Protein expression was determined by flow cytometry. In some cases, sorting for high expressing cells was performed using the FACSaria Fusion flow cytometer.

#### CMV infection of fibroblasts

In order to ensure comparable conditions with confluent layers of infected and noninfected cells as well as a high degree of well infected and stressed cells, we performed a multistep infection protocol. The HCMV strain used in this study is the TB40R virus described recently (Hammer et al., 2018). In brief, hTERT-BJ-1 were infected with TB40R at a multiplicity of infection of 0.1 and cultured until 100% of visible cytopathic effect was reached. To further increase the frequency of living CMV<sup>+</sup> cells, infected and noninfected hTERT-BJ-1 were mixed at a ratio of 1:3, incubated for 3 d, trypsinized, and seeded into 96-well plates to be used for the experiments 4 d later. The seeding density for confluent cell layers was 20,000 of infected or 10,000 of noninfected cells per well of a 96-well plate, as the infected cells were more susceptible to cell death.

#### Coculture of JE6.1 reporter cells with target cell lines

JE6.1 reporter cell lines expressing the investigated  $\gamma\delta$  TCRs were harvested and brought to a density of  $1 \times 10^6$  ml<sup>-1</sup> with RPMI culture medium without antibiotics. The suspension target cell lines Raji and derivatives, K562, U937, BL64, KG-1, THP-1, and CEM were harvested and prestained with the cell proliferation dye eFluor 670 (Invitrogen) according to the manufacturer's protocol to allow for distinction of target versus reporter cells in flow cytometry. Target and reporter cells were cocultured at a ratio of 1:1 with  $5 \times 10^4$  cells on both sides. For coculture with CMV-infected fibroblasts, medium was taken off and the fibroblasts were washed once with PBS. Afterwards,  $5 \times 10^4$  reporter cells were added to the respective wells. The coculture volume was 100  $\mu$ l in a 96-well plate. The negative control were reporter cells without target cells and the positive control were beads coated with anti-CD3/anti-CD28 antibodies (Treg Expansion Kit; Miltenyi) for the stimulation of TCR signaling. The cells were cocultured overnight, and the GFP fluorescence was detected the next day via flow cytometry.

#### Coculture with primary B cells

Frozen PBMCs from patients or healthy donors were thawed and counted. The cells were stained with antibodies for CD3, CD19, and HLA-DR as described above and sorted for CD19<sup>+</sup>/CD3<sup>-</sup> cells with the FACSaria Fusion at the Cell Sorting Facility of Hannover Medical School. The obtained B cells were counted, and the JE6.1 reporter cell lines were counted and added in a ratio of 1:1 as described in the previous section. After culturing the cells together overnight, the samples were again stained with anti-CD19 antibody and DAPI as described above to separate B cells from JE6.1 cells. The GFP fluorescence was then detected via flow cytometry.

#### Stimulation of fibroblasts with IFN- $\gamma$

$5 \times 10^4$  hTERT-BJ-1 cells were seeded into wells of a 96-well plate in culture medium and left overnight to allow for attachment. 25 ng/ $\mu$ l IFN- $\gamma$  was added for 24 h and subsequently removed by washing with RPMI coculture medium. HLA-DR expression was determined via flow cytometry and a coculture with JE6.1 reporter cells was performed as described above.

#### Protein expression and purification

For expression and purification of soluble HLA-DR, the transmembrane regions of the DRA1 chain and the DRB1\*03 chain were replaced with the leucine zipper dimerization motifs from the transcription factors Fos and Jun, respectively, following a similar strategy as used previously for HLA-DR2 (Kalandadze et al., 1996). FusionRed-MV and a double strep-tag were added to the C-terminus of DRB1 3, and a CLIP peptide was covalently linked to the N-terminus of the DRB1-3 chain via a  $3 \times$  GGGGS-linker. The corresponding genes were cloned into the vector pT1205 for expression in *Drosophila* S2 cells as described previously (Krey et al., 2010). A stable S2 transfectant was established and the protein produced as described previously (Johansson et al., 2012) with minor method modifications. Briefly, a total of 2- $\mu$ g plasmid (1:1 ratio) was cotransfected with 0.1- $\mu$ g pCoPuro plasmid (Iwaki et al., 2003). Following a 6-d

selection period, stable cell lines were then adapted to insect-Xpress media (Lonza). For large-scale production, cells were induced with 4-mM CdCl<sub>2</sub> at a density of 7 × 10<sup>6</sup> cells/ml for 5 d, pelleted, and the soluble HLA was purified by affinity chromatography from the supernatant using a Strep-Tactin XT 4Flow column (IBA Lifesciences) followed by size exclusion chromatography using a HiLoad 26/600 superdex 200 pg column (Cytiva) equilibrated in 20-mM Hepes, pH 7.4, and 150-mM NaCl. For expression and purification of soluble TCRs, stable S2 transfectants were generated for TCR02, TCR04 and TCR05 as described earlier for HLA-DR, and a similar protocol was followed for expression of recombinant sTCR. For binding analyses, the affinity tags were proteolytically removed using enterokinase according to the manufacturer's recommendation.

### Surface plasmon resonance

To determine the HLA-CLIP- γδ TCR-binding specificity and affinity constants, surface plasmon resonance was performed with the BIAcore X-100 system (Cytiva; previously GE Healthcare) as described previously (González-Motos et al., 2017). Experiments were performed at 25°C using HBS-EP (0.01 M Hepes, pH 7.5, 0.15 M NaCl, 3 mM EDTA, 0.05% Tween20) as running buffer. On both flow cells of a CM5 chip (Cytiva) about 1,500 response units (RU) StrepTactinXT (Twin-Strep-tag Capture Kit from IBA) were immobilized via amine coupling using acetate buffer, pH 4.5 (amine coupling kit from GE Healthcare). Twin-Strep-tagged HLA-CLIP was captured on FC2 and the TCRs were injected into both flow cells. For binding assays, analytes were injected at 2.5 μM for 90 s followed by 60 s of dissociation with a flow rate of 10 μl/min. For single-cycle kinetics, the contact time was increased to 120 s and the dissociation time to 90 s with a flow rate of 30 μl/min. To regenerate the StrepTactinXT surface, 3-M GuHCl was injected for 60 s. All analyses were performed with the Biacore x100 Evaluation Software. The sensorgrams of FC2-1 were adjusted and a blank injection was subtracted. For kinetic analyses, data were fitted using a 1:1 binding model.

### sTCR staining

For tetramerization with streptavidin-PE (Invitrogen), the ratio of sTCR:streptavidin-PE was 4:1. 4.07-μg sTCR were added to 4-μl streptavidin-PE and incubated for 45 min on ice. Afterwards, 1.325 μl of the tetramer suspension was used to stain up to 1 × 10<sup>6</sup> cells per sample in PBS + 1% FCS. After 20 min on ice, the cells were washed once with PBS + 1% FCS and the fluorescence detected by flow cytometry.

### Genome-wide CRISPR/Cas9 knockout screening

In order to identify the antigen for TCR04 and TCR05, a genome-wide knockout screening with the Raji cell line was performed. The Human Brunello CRISPR knockout pooled library was a gift from David Root and John Doench (#73178; Addgene). The transduction of the library was performed as described in Doench et al. (2016). In brief, the library was obtained as a prepacked virus suspension and transduced into Raji cells with an infection efficiency of ~40% to reach a multiplicity of infection of 0.5–1 and selected with 1 ng/μl of puromycin for 5 d. Half of every sample was directly submitted to genomic DNA

isolation and the other half was stained with sTCR tetramers as stated above. The lowest 10% of the stained cells were sorted and cultured for 1 wk in RPMI culture medium. The staining and sorting procedures were repeated three more times to accumulate the sTCR negative cells. Genomic DNA was isolated from the sorted cells and the sgRNA sequences were PCR-amplified according to a protocol provided with the sgRNA library by David Root and John Doench. The PCR library was subsequently sequenced by Illumina NovaSeq at CeGaT. After quality control and trimming, the stagger included in the sequencing primers was removed using the *cutadapt* function (Martin, 2011). Bioinformatic analysis for the identification of enriched sgRNAs was performed with the edgeR package in R (Robinson et al., 2010). In brief, the reads were annotated and counted using the *processAmplicons* function with tolerance for single base pair mismatches and/or shifted guide positions. With the application of a threshold of 0.5 counts per 10<sup>6</sup> reads, sequencing errors were excluded. In the case of single-cell clone-derived samples, the first 1–3 sgRNAs of the resulting list were representing the majority of all sequences and were therefore considered as the relevant hits. sgRNAs that were accumulated in the sorted replicates were identified with the *exactTest* function. Increased sgRNAs showing a log-fold change from unsorted to sorted of >1, a P value <0.05 and a false discovery rate of <0.0001 were considered as significant.

### HLA-DR tetramer staining

Biotinylated HLA-DRB1\*03 containing the CMV-specific peptides (sequence IE1) and (sequence IE2) were obtained from immunAware. Tetramerization was performed according to manufacturer's instructions by adding one fourth of the molar amount of streptavidin-PE or streptavidin-APC and incubate for 45 min in total. The remaining tetramers were purchased ready to use from ProImmune. The tetramers were added either to JE6.1 cells expressing TCR02, TCR04, or TCR05 in RPMI culture medium and incubated for 1 h at 37°C. Next, the cells were washed once and stained with the respective antibodies in PBS with 1% FCS as described above.

For staining PBMCs, γδ T cells were specifically enriched via MACS isolation using the TCRg/d<sup>+</sup> T cell isolation kit human from Miltenyi and the autoMACS separator and the obtained cells were resuspended in RPMI culture medium. Tetramers labeled with APC and PE were mixed 1:1 and added to the MACS-isolated γδ T cells according to the manufacturer's instructions. The cells were stained for 1 h at 37°C, washed once, and stained with the respective antibodies in PBS with 1% FCS as described above.

### Determination of HLA-DRB haplotype by Illumina Sequencing

RNA isolation of the cell lines Raji, BL64 and KG-1 was performed using the RNeasy Plus Mini Kit (250) from Qiagen according to manufacturer's instructions. Next, cDNA was synthesized using the Superscript III Reverse Transcriptase Kit from Invitrogen. A 399-bp-long fragment covering exon 2 of HLA-DRB was amplified using the NEBNext 2× PCR Master Mix from New England Biolabs. In a second PCR step, the Illumina flow cell binding site and indices for demultiplexing were added

to the amplicons using the Advantage 2 Polymerase from Clontech. Subsequent purification of the PCR products was performed with the Agencourt AMPure XP PCR Purification Kit (Beckman Coulter) according to manufacturer's instructions. For Illumina Sequencing, the MiSeq V2 Reagent Kit was used with  $2 \times 250$  cycles on a MiSeq machine.

### Single-cell gene expression and $\gamma\delta$ TCR analysis

For single-cell  $\gamma\delta$  TCR and gene expression (GEX) analysis,  $\gamma\delta$  T cells from frozen PBMCs were isolated by FACS sorting based on expression of CD3 (anti-CD3 FITC) and TCR $\gamma\delta$  (anti-TCR $\gamma\delta$ -PE), dead cells (DAPI+), and TCR $\beta$ + (anti-TCR $\beta$ -APCVio770)  $\alpha\beta$  T cells were excluded from analysis. Prior to FACS sorting, PBMCs were thawed and rested in medium for  $\sim 1$  h at  $37^\circ\text{C}$  and 5%  $\text{CO}_2$ .  $\gamma\delta$  T cells were sorted into DNA low binding tubes containing PBS with 3% FCS. After sorting,  $\gamma\delta$  T cells from indicated time points, post-HSCT were mixed in a 1:1 ratio. In order to discriminate cells from different time points, post-HSCT TotalSeq-C Hashtag antibodies (Biolegend) were used with 0.1  $\mu\text{g}$  antibody/ $1 \times 10^6$  cells in 100  $\mu\text{l}$  PBS 1% BSA. Labeling of the PBMCs with Hashtag antibodies was performed together with fluorochrome-labeled antibodies prior to FACS sort according to manufacturer's instructions (Biolegend). Sorted  $\gamma\delta$  T cells were loaded on a Chromium Next GEM Chip G (10xGenomics) according to manufacturer's instructions. cDNA and subsequently GEX and  $\gamma\delta$  TCR libraries were generated using 10xGenomics Chromium Next GEM Single Cell V(D)J Reagent Kits V1.1 according to manufacturer's instructions. V(D)J enrichment was facilitated using custom primers for  $\gamma\delta$  T cells: h\_gd-Fwd-1: 5'-AATGATACGGCGACCACCGAGATCTACACTCTTTCCCTACACGACGCTC-3'; h\_gd-TRD-1: 5'-CCCCTGGGAGAGATGACAA-3'; h\_gd-TRG-1: 5'-ATCCCAGAATCGTGTGCTC-3'; h\_gd-Fwd-2: 5'-AATGATACGGCGACCACCGAGATCT-3'; h\_gd-TRD-2: 5'-GACAAAACGGATGTTTGG-3'; h\_gd-TRG-2: 5'-GGGGAAACATCTGCATCAAG-3'.

Libraries were sequenced on a NextSeq Illumina Sequencer with the following parameters: SRI:26bp, IR:8bp, SR2: 134bp.

The single-cell GEX and TCR analysis were done according to the same protocol, as described in Tan et al. (2021). Briefly, single-cell GEX and TCR were aligned and annotated to human reference genome GRCh38 using 10xGenomics Cellranger v3.0. Annotated GEX and TCR metrics were exported to R v4.0 and analyzed by Seurat v4.0. After log-normalization, GEX metric was supplied to principal component analysis for dimensional reduction, and then embedded by Uniform Manifold Approximation and Projection (UMAP) for visualization. Single-cell GEX and TCR were paired by the cellular barcodes.

### Trogocytosis assay

The staining of Raji cells with eFluor 670 was performed as described above for cocultures. To detect transfer of cell surface proteins from Raji to JE6.1 cells upon  $\gamma\delta$  TCR activation, Raji cells were biotinylated on the cell surface by using EZ-Link Sulfo-NHS-LC-Biotin from Thermo Fisher Scientific according to manufacturer's instructions. In brief, the cells were washed three times with PBS and EZ-Link Sulfo-NHS-LC-Biotin was added at a concentration of 2 mM. After 30 min of incubation at

room temperature, the cells were washed three times with RPMI culture medium without antibiotics and the  $5 \times 10^4$  cells were added to the respective wells of a 96-well plate. JE6.1 cells were added at a ratio of 1:1 and cells were incubated for 5 min at  $37^\circ\text{C}$ . After a washing step with PBS + 1% FCS, the cells were stained with streptavidin-APC (Invitrogen) at a dilution of 1:250 and the detection was performed by flow cytometry.

The specific transfer of HLA-DR was measured by antibody staining against HLA-DR and CD19. In brief, unstained Raji and JE6.1 cells were cocultured at a ratio of 1:1 for 5 min and subsequently stained for HLA-DR and CD19 for separation of Raji and JE6.1 cells. Detection was again performed by flow cytometry.

### Statistical analysis

The indicated statistical tests to compare datasets have been performed in GraphPad Prism 8.

### Online supplemental material

Fig. S1 shows the expression of transduced  $\gamma\delta$  TCRs in JE6.1 cells. Fig. S2 A shows the HLA-DR expression before and after the CRISPR/Cas9-mediated gene repair, and Fig. S2 B shows the coculture results of  $\gamma\delta$  TCR-expressing JE6.1 reporter cells with either Raji WT or Raji RFXAP knockout cells (*RFXAP*<sup>-/-</sup>) transduced with HLA-DRA and indicated HLA-DRB. Fig. S3 shows a staining of  $\gamma\delta$  TCR-expressing JE6.1 reporter cells with HLA-DR tetramers presenting different peptides. Table S1 includes the Top 20 increased sgRNAs from genome-wide CRISPR/Cas9 screening. Table S2 shows the HLA-DRB haplotypes of HLA-DR-expressing cell lines.

### Data availability

Raw data of the single-cell sequencing (Fig. 1, A–C) and the genome-wide CRISPR/Cas9 knockout screening (Fig. 2, C and D) are available on the SRA database under the accession PRJNA771240 and project title "Identification of HLA-DR as an antigen for a Vdelta1-positive gamma-delta TCR." All necessary data to understand and evaluate the conclusions of this paper are provided in the manuscript and supplemental material.

### Acknowledgments

We thank M. Ballmeier for support from the cell-sorting core facility of Hannover Medical School. Furthermore, we thank B. Bosnjak for providing scientific and technical advice for the generation of CRISPR/Cas9 knockout cell lines and gene repair experiments. We also thank A. Fichtner, E. Bruni, and M. Stieger for helping with the isolation of PBMCs.

This work was supported by the Deutsche Forschungsgemeinschaft (DFG; German Research Foundation) Research Unit FOR 2799 to I. Prinz (Project PR727/11-1) and T. Krey; grant CRC SFB900 (Project ID 158989968) to C. Koenecke and I. Prinz; and under Germany's Excellence Strategy (EXC 2155 "RESIST"), Project ID 390874280 to A.V. Borbolla, M. Messerle, T. Krey, and I. Prinz. M. Deseke, G.L. Ssebyatika, C. Jürgens, N. Plückerbaum, and A. Hassan were supported by the Hannover Biomedical Research School and Zentrum für Infektionsbiologie; C. Jürgens

was supported by a DFG grant from the DFG, VI 762/1-1, Project ID 405772731.

Author contributions: Conceptualization: I. Prinz, T. Krey, M. Deseke. Methodology: I. Prinz, T. Krey, M. Deseke, M. Messerle. Investigation: M. Deseke, F. Rampoldi, I. Sandrock, C. Jürgens, N. Plückerbaum, M. Beck, A. Hassan, A. Demera, A. Janssen. Sequencing data analysis: M. Deseke, L. Tan. Resources: E. Borst, H. Böning, G.L. Ssebyatika, P. Steinberger, C. Koenecke. Supervision: I. Prinz, T. Krey. Writing—original draft: M. Deseke, I. Prinz. Writing—review and editing: M. Deseke, I. Prinz, F. Rampoldi, I. Sandrock, C. Jürgens, N. Plückerbaum, L. Tan, P. Steinberger, C. Koenecke, A.V. Borbolla, M. Messerle, T. Krey. Funding acquisition: I. Prinz, C. Koenecke, T. Krey, M. Messerle, A.V. Borbolla.

Disclosures: M. Deseke and I. Prinz reported a patent to ASC 15-00694 issued. No other disclosures were reported.

Submitted: 20 December 2021

Revised: 2 June 2022

Accepted: 30 June 2022

## References

- Benveniste, P.M., S. Roy, M. Nakatsugawa, E.L.Y. Chen, L. Nguyen, D.G. Millar, P.S. Ohashi, N. Hirano, E.J. Adams, and J.C. Zúñiga-Pflücker. 2018. Generation and molecular recognition of melanoma-associated antigen-specific human  $\gamma\delta$  T cells. *Sci. Immunol.* 3:eav4036. <https://doi.org/10.1126/sciimmunol.aav4036>
- Ciccione, E., O. Viale, D. Pende, M. Malnati, G. Battista Ferrara, S. Barocci, A. Moretta, and L. Moretta. 1989. Specificity of human T lymphocytes expressing a gamma/delta T cell antigen receptor. Recognition of a polymorphic determinant of HLA class I molecules by a gamma/delta clone. *Eur. J. Immunol.* 19:1267–1271. <https://doi.org/10.1002/eji.1830190718>
- Crivello, P., M. Ahci, F. Maaßen, N. Wossidlo, E. Arrieta-Bolaños, A. Heinold, V. Lange, J.H.F. Falkenburg, P.A. Horn, K. Fleischhauer, and S. Heinrichs. 2019. Multiple knockout of classical HLA class II  $\beta$ -chains by CRISPR/Cas9 genome editing driven by a single guide RNA. *J. Immunol.* 202:1895–1903. <https://doi.org/10.4049/jimmunol.1800257>
- Davey, M.S., C.R. Willcox, S.P. Joyce, K. Ladell, S.A. Kasatskaya, J.E. McLaren, S. Hunter, M. Salim, F. Mohammed, D.A. Price, et al. 2017. Clonal selection in the human V $\delta$ 1 T cell repertoire indicates  $\gamma\delta$  TCR-dependent adaptive immune surveillance. *Nat. Commun.* 8:14760. <https://doi.org/10.1038/ncomms14760>
- Delfau, M.H., A.J. Hance, D. Lecossier, E. Vilmer, and B. Grandchamp. 1992. Restricted diversity of V gamma 9-JP rearrangements in unstimulated human gamma/delta T lymphocytes. *Eur. J. Immunol.* 22:2437–2443. <https://doi.org/10.1002/eji.1830220937>
- Del Porto, P., M. D'Amato, M.T. Fiorillo, L. Tuosto, E. Piccolella, and R. Sorrentino. 1994. Identification of a novel HLA-B27 subtype by restriction analysis of a cytotoxic gamma delta T cell clone. *J. Immunol.* 153:3093–3100.
- Deseke, M., and I. Prinz. 2020. Ligand recognition by the  $\gamma\delta$  TCR and discrimination between homeostasis and stress conditions. *Cell Mol. Immunol.* 17:914–924. <https://doi.org/10.1038/s41423-020-0503-y>
- Doench, J.G., N. Fusi, M. Sullender, M. Hegde, E.W. Vaimberg, K.F. Donovan, I. Smith, Z. Tothova, C. Wilen, R. Orchard, et al. 2016. Optimized sgRNA design to maximize activity and minimize off-target effects of CRISPR-Cas9. *Nat. Biotechnol.* 34:184–191. <https://doi.org/10.1038/nbt.3437>
- Fichtner, A.S., S. Ravens, and I. Prinz. 2020. Human  $\gamma\delta$  TCR repertoires in health and disease. *Cells.* 9:800. <https://doi.org/10.3390/cells9040800>
- Flament, C., A. Benmerah, M. Bonneville, F. Triebel, and F. Mami-Chouaib. 1994. Human TCR-gamma/delta alloreactive response to HLA-DR molecules. Comparison with response of TCR-alpha/beta. *J. Immunol.* 153:2890–2904
- González-Motos, V., C. Jürgens, B. Ritter, K.A. Kropp, V. Durán, O. Larsen, A. Binz, W.J.D. Ouwendijk, T. Lenac Rovis, S. Jonjic, et al. 2017. Varicella zoster virus glycoprotein C increases chemokine-mediated leukocyte migration. *PLoS Pathog.* 13:e1006346. <https://doi.org/10.1371/journal.ppat.1006346>
- Hammer, Q., T. Rückert, E.M. Borst, J. Dunst, A. Haubner, P. Durek, F. Heinrich, G. Gasparoni, M. Babic, A. Tomic, et al. 2018. Peptide-specific recognition of human cytomegalovirus strains controls adaptive natural killer cells. *Nat. Immunol.* 19:453–463. <https://doi.org/10.1038/s41590-018-0082-6>
- Harly, C., S.P. Joyce, C. Domblides, T. Bachelet, V. Pitard, C. Mannat, A. Pappalardo, L. Couzi, S. Netzer, L. Massara, et al. 2021. Human  $\gamma\delta$  T cell sensing of AMPK-dependent metabolic tumor reprogramming through TCR recognition of EphA2. *Sci. Immunol.* 6:eaba9010. <https://doi.org/10.1126/sciimmunol.aba9010>
- Iwaki, T., M. Figuera, V.A. Ploplis, and F.J. Castellino. 2003. Rapid selection of *Drosophila* S2 cells with the puromycin resistance gene. *Biotechniques.* 35:482–484, 486. <https://doi.org/10.2144/033535bm08>
- Johansson, D.X., T. Krey, and O. Andersson. 2012. Production of recombinant antibodies in *drosophila melanogaster* s2 cells. *Methods Mol. Biol.* 907:359–370. [https://doi.org/10.1007/978-1-61779-974-7\\_21](https://doi.org/10.1007/978-1-61779-974-7_21)
- Kalandadze, A., M. Galleno, L. Foncerrada, J.L. Strominger, and K.W. Wucherpfennig. 1996. Expression of recombinant HLA-DR2 molecules: Replacement of the hydrophobic transmembrane region by a leucine zipper dimerization motif allows the assembly and secretion of soluble DR  $\alpha\beta$  heterodimers. *J. Biol. Chem.* 271:20156–20162. <https://doi.org/10.1074/jbc.271.33.20156>
- Karunakaran, M.M., C.R. Willcox, M. Salim, D. Paletta, A.S. Fichtner, A. Noll, L. Starick, A. Nöhren, C.R. Begley, K.A. Berwick, et al. 2020. Butyrophilin-2A1 directly binds germline-encoded regions of the V $\gamma$ 9V $\delta$ 2 TCR and is essential for phosphoantigen sensing. *Immunity.* 52:487–498.e6. <https://doi.org/10.1016/j.immuni.2020.02.014>
- Kierkels, G.J.J., W. Scheper, A.D. Meringa, I. Johanna, D.X. Beringer, A. Janssen, M. Schiffler, T. Aarts-Riemens, L. Kramer, T. Straetmans, et al. 2019. Identification of a tumor-specific allo-HLA-restricted  $\gamma\delta$ TCR. *Blood Adv.* 3:2870–2882. <https://doi.org/10.1182/bloodadvances.2019032409>
- Krey, T., J. D'Alayer, C.M. Kikuti, A. Saulnier, L. Damier-Piolle, I. Petitpas, D.X. Johansson, R.G. Tawar, B. Baron, B. Robert, et al. 2010. The disulfide bonds in glycoprotein E2 of hepatitis C virus reveal the tertiary organization of the molecule. *PLoS Pathog.* 6:e1000762. <https://doi.org/10.1371/journal.ppat.1000762>
- Legut, M., G. Dolton, A.A. Mian, O.G. Ottmann, and A.K. Sewell. 2018. CRISPR-mediated TCR replacement generates superior anticancer transgenic T-cells. *Blood.* 131:311–322. <https://doi.org/10.1182/blood-2017-05-787598>
- le Nours, J., N.A. Gherardin, S.H. Ramarathinam, W. Awad, F. Wiede, B.S. Gully, Y. Khandokar, T. Praveena, J.M. Wubben, J.J. Sandow, et al. 2019. A class of  $\gamma\delta$  T cell receptors recognize the underside of the antigen-presenting molecule MRI. *Science.* 366:1522–1527. <https://doi.org/10.1126/science.aav3900>
- Li, G., M.T. Bethune, S. Wong, A.V. Joglekar, M.T. Leonard, J.K. Wang, J.T. Kim, D. Cheng, S. Peng, J.M. Zaretsky, et al. 2019. T cell antigen discovery via trogocytosis. *Nat. Methods.* 16:183–190. <https://doi.org/10.1038/s41592-018-0305-7>
- Liuzzi, A.R., J.E. McLaren, D.A. Price, and M. Eberl. 2015. Early innate responses to pathogens: Pattern recognition by unconventional human T-cells. *Curr. Opin. Immunol.* 36:31–37. <https://doi.org/10.1016/j.coi.2015.06.002>
- Marlin, R., A. Pappalardo, H. Kaminski, C.R. Willcox, V. Pitard, S. Netzer, C. Khairallah, A.-M. Lomenech, C. Harly, M. Bonneville, et al. 2017. Sensing of cell stress by human  $\gamma\delta$  TCR-dependent recognition of annexin A2. *Proc. Natl. Acad. Sci. USA.* 114:3163–3168. <https://doi.org/10.1073/pnas.1621052114>
- Martens, R., M. Permanyer, K. Werth, K. Yu, A. Braun, O. Halle, S. Halle, G.E. Patzer, B. Bošnjak, F. Kiefer, et al. 2020. Efficient homing of T cells via afferent lymphatics requires mechanical arrest and integrin-supported chemokine guidance. *Nat. Commun.* 11:1114. <https://doi.org/10.1038/s41467-020-14921-w>
- Martin, M. 2011. Cutadapt removes adapter sequences from high-throughput sequencing reads. *EMBnet J.* 17:10. <https://doi.org/10.14806/ej.17.1.200>
- Maurer, D.H., J.H. Hanke, E. Mickelson, R.R. Rich, and M.S. Pollack. 1987. Differential presentation of HLA-DR, DQ, and DP restriction elements by interferon- $\gamma$ -treated dermal fibroblasts. *J. Immunol.* 139:715–723.
- Melandri, D., I. Zlatareva, R.A.G. Chaleil, R.J. Dart, A. Chancellor, O. Nussbaumer, O. Polyakova, N.A. Roberts, D. Wesch, D. Kabelitz, et al. 2018. The  $\gamma\delta$ TCR combines innate immunity with adaptive immunity by

- utilizing spatially distinct regions for agonist selection and antigen responsiveness. *Nat. Immunol.* 19:1352–1365. <https://doi.org/10.1038/s41590-018-0253-5>
- Morita, C.T., C. Jin, G. Sarikonda, and H. Wang. 2007. Nonpeptide antigens, presentation mechanisms, and immunological memory of human Vgamma2Vdelta2 T cells: Discriminating friend from foe through the recognition of prenyl pyrophosphate antigens. *Immunol. Rev.* 215:59–76. <https://doi.org/10.1111/j.1600-065X.2006.00479.x>
- Ravens, S., A.S. Fichtner, M. Willers, D. Torkornoo, S. Pirr, J. Schöning, M. Deseke, I. Sandrock, A. Bubke, A. Wilharm, et al. 2020. Microbial exposure drives polyclonal expansion of innate  $\gamma\delta$  T cells immediately after birth. *Proc. Natl. Acad. Sci. USA.* 117:18649–18660. <https://doi.org/10.1073/pnas.1922588117>
- Ravens, S., C. Schultze-Florey, S. Raha, I. Sandrock, M. Drenker, L. Oberdörfer, A. Reinhardt, I. Ravens, M. Beck, R. Geffers, et al. 2017. Human  $\gamma\delta$  T cells are quickly reconstituted after stem-cell transplantation and show adaptive clonal expansion in response to viral infection. *Nat. Immunol.* 18:393–401. <https://doi.org/10.1038/ni.3686>
- Rigau, M., S. Ostrouska, T.S. Fulford, D.N. Johnson, K. Woods, Z. Ruan, H.E.G. McWilliam, C. Hudson, C. Tutuka, A.K. Wheatley, et al. 2020. Butyrophilin 2A1 is essential for phosphoantigen reactivity by  $\gamma\delta$  T cells. *Science.* 367:eaay5516. <https://doi.org/10.1126/science.aay5516>
- Robinson, M.D., D.J. McCarthy, and G.K. Smyth. 2010. edgeR: A Bioconductor package for differential expression analysis of digital gene expression data. *Bioinformatics.* 26:139–140. <https://doi.org/10.1093/bioinformatics/btp616>
- Roskopf, S., S. Jutz, A. Neunkirchner, M.R. Candia, B. Jahn-Schmid, B. Bohle, W.F. Pickl, and P. Steinberger. 2016. Creation of an engineered APC system to explore and optimize the presentation of immunodominant peptides of major allergens. *Sci. Rep.* 6:31580. <https://doi.org/10.1038/srep31580>
- Roy, S., D. Ly, C.D. Castro, N.-S. Li, A.J. Hawk, J.D. Altman, S.C. Meredith, J.A. Piccirilli, D.B. Moody, and E.J. Adams. 2016. Molecular analysis of lipid-reactive V $\delta$ 1  $\gamma\delta$  T cells identified by CD1c tetramers. *J. Immunol.* 196:1933–1942. <https://doi.org/10.4049/jimmunol.1502202>
- Russano, A.M., E. Agea, L. Corazzi, A.D. Postle, G. De Libero, S. Porcelli, F.M. de Benedictis, and F. Spinozzi. 2006. Recognition of pollen-derived phosphatidyl-ethanolamine by human CD1d-restricted gamma delta T cells. *J. Allergy Clin. Immunol.* 117:1178–1184. <https://doi.org/10.1016/j.jaci.2006.01.001>
- Sandstrom, A., C.M. Peigné, A. Léger, J.E. Crooks, F. Konczak, M.C. Gesnel, R. Breathnach, M. Bonneville, E. Scotet, and E.J. Adams. 2014. The intracellular B30.2 domain of butyrophilin 3A1 binds phosphoantigens to mediate activation of human V $\gamma$ 9V $\delta$ 2 T Cells. *Immunity.* 40:490–500. <https://doi.org/10.1016/j.immuni.2014.03.003>
- Scheper, W., S. van Dorp, S. Kersting, F. Pietersma, C. Lindemans, S. Hol, S. Heijhuurs, Z. Sebestyen, C. Gründer, V. Marcu-Malina, et al. 2013.  $\gamma\delta$  T cells elicited by CMV reactivation after allo-SCT cross-recognize CMV and leukemia. *Leukemia.* 27:1328–1338. <https://doi.org/10.1038/leu.2012.374>
- Tan, L., A.S. Fichtner, E. Bruni, I. Odak, I. Sandrock, A. Bubke, A. Borchers, C. Schultze-Florey, C. Koenecke, R. Förster, et al. 2021. A fetal wave of human type 3 effector  $\gamma\delta$  cells with restricted TCR diversity persists into adulthood. *Sci. Immunol.* 6:eabf0125. <https://doi.org/10.1126/sciimmunol.abf0125>
- Uldrich, A.P., J. le Nours, D.G. Pellicci, N.A. Gherardin, K.G. McPherson, R.T. Lim, O. Patel, T. Beddoe, S. Gras, J. Rossjohn, and D.I. Godfrey. 2013. CD1d-lipid antigen recognition by the  $\gamma\delta$  TCR. *Nat. Immunol.* 14:1137–1145. <https://doi.org/10.1038/ni.2713>
- Wang, H., Z. Fang, and C.T. Morita. 2010. Vgamma2Vdelta2 T cell receptor recognition of prenyl pyrophosphates is dependent on all CDRs. *J. Immunol.* 184:6209–6222. <https://doi.org/10.4049/jimmunol.1000231>
- Willcox, B.E., and C.R. Willcox. 2019.  $\gamma\delta$  TCR ligands: The quest to solve a 500-million-year-old mystery. *Nat. Immunol.* 20:121–128. <https://doi.org/10.1038/s41590-018-0304-y>
- Willcox, C.R., V. Pitard, S. Netzer, L. Couzi, M. Salim, T. Silberzahn, J.-F. Moreau, A.C. Hayday, B.E. Willcox, and J. Déchanet-Merville. 2012. Cytomegalovirus and tumor stress surveillance by binding of a human  $\gamma\delta$  T cell antigen receptor to endothelial protein C receptor. *Nat. Immunol.* 13:872–879. <https://doi.org/10.1038/ni.2394>
- Xiao, L., C. Chen, Z. Li, S. Zhu, J.C. Tay, X. Zhang, S. Zha, J. Zeng, W.K. Tan, X. Liu, et al. 2018. Large-scale expansion of V $\gamma$ 9V $\delta$ 2 T cells with engineered K562 feeder cells in G-Rex vessels and their use as chimeric antigen receptor-modified effector cells. *Cytotherapy.* 20:420–435. <https://doi.org/10.1016/j.jcyt.2017.12.014>

## Supplemental material

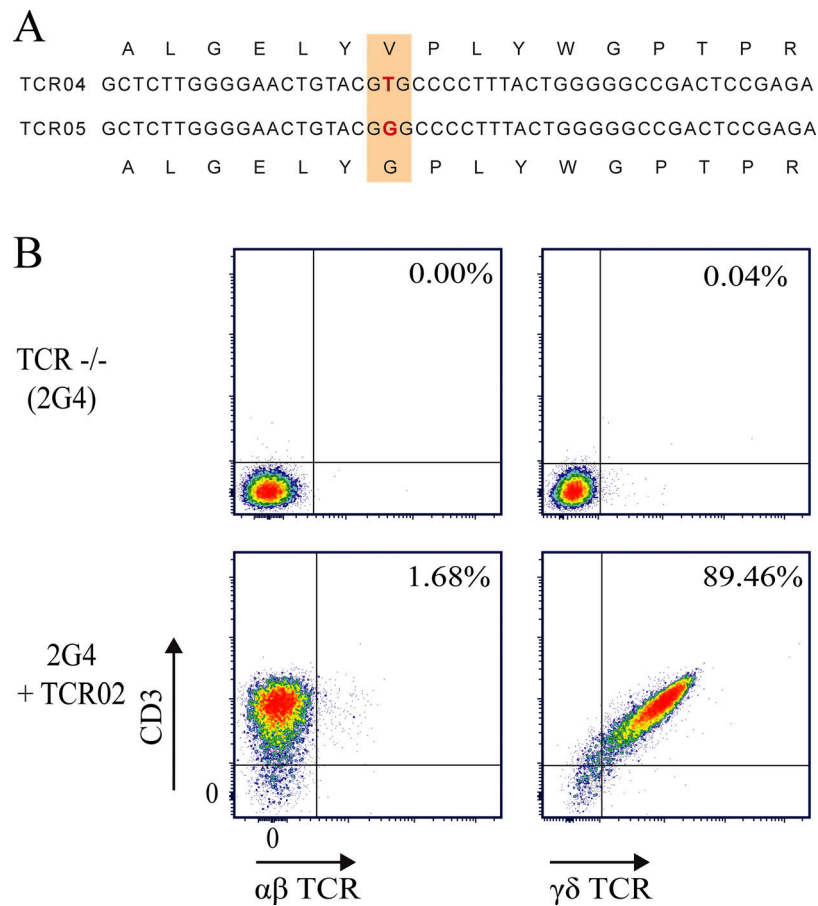


Figure S1. **Functional γδ TCR expression in JE6.1 reporter cells.** (A) Alignment of nucleotide sequences of the CDR3 of TCR04 and TCR05 as identified in the original γδ TCR repertoire study. (B) Staining of JE6.1 cells for expression of CD3, αβ TCR, and γδ TCR. 2G4: TCR β knockout clone.

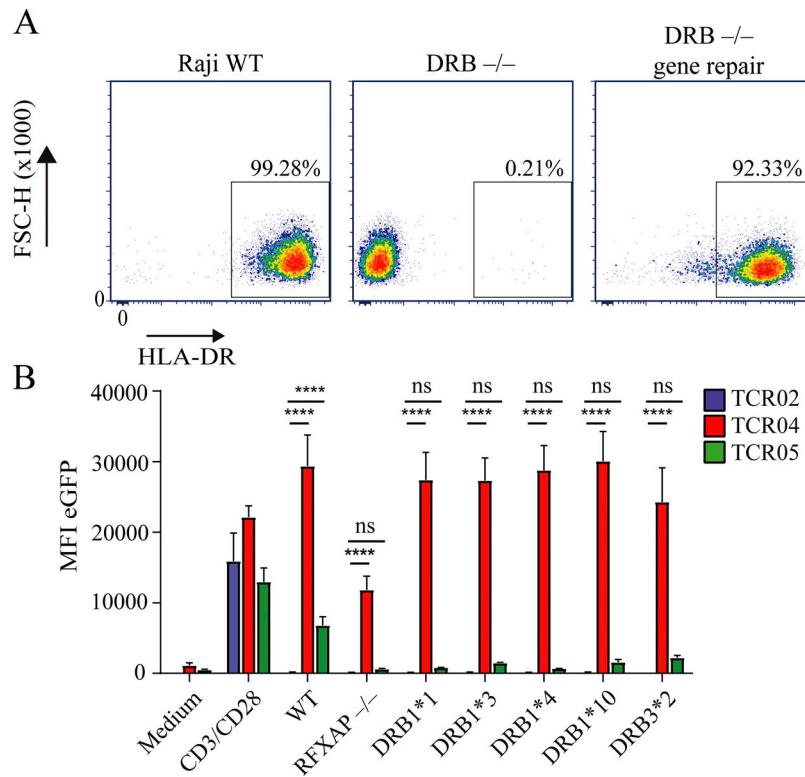


Figure S2. **Reconstitution of HLA-DR expression by transduction and gene repair.** (A) Staining for HLA-DR expression of Raji WT cells as positive control, Raji DRB knockout cells (DRB<sup>-/-</sup>) treated with sgRNA, and a nonspecific DNA oligomer and DRB<sup>-/-</sup> cells treated with sgRNA and specific DNA oligo with sequences homologous to target site (DRB<sup>-/-</sup> gene repair). (B) GFP fluorescence of JE6.1 reporter cells expressing the respective  $\gamma\delta$  TCRs with either Raji WT, Raji RFXAP knockout cells (RFXAP<sup>-/-</sup>) or RFXAP<sup>-/-</sup> transduced with HLA-DRA and indicated HLA-DRB. Statistical test: two-way ANOVA with Tukey's multiple comparisons test; \*\*\*\*,  $P < 0.0001$  ( $n = 3$ , error bars = SD of mean).



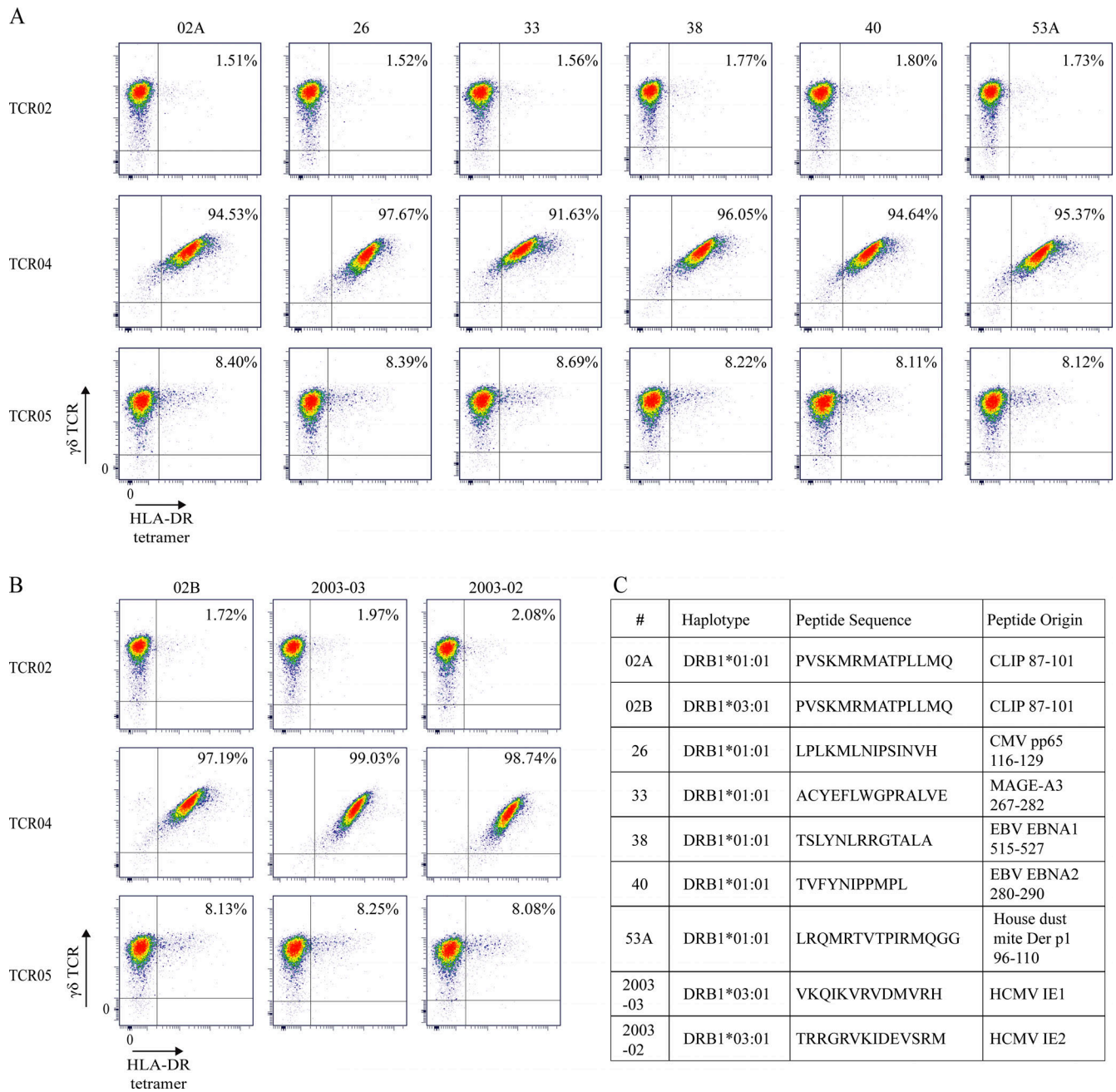


Figure S3. Staining of JE6.1 cells expressing TCR02, TCR04, or TCR05 with different HLA-DR tetramers. (A and B) The reporter cells were stained with HLA-DR tetramers of the haplotype DRB1\*1 (A) or DRB1\*3 (B). (C) The peptides presented by the tetramers are listed in C.

Provided online are two tables. Table S1 includes the Top 20 increased sgRNAs from genome-wide CRISPR/Cas9 screening. Table S2 shows the HLA-DRB-haplotypes of HLA-DR-expressing cell lines.